MECHANOCHEMISTRY AND MECHANICAL ALLOYING 2003
JOURNAL OF MATERIALS SCIENCE **39** (2004) 5451–5453

Mechanochemically activated nano-aluminium: Oxidation behaviour

A. PIVKINA*, A. STRELETSKII, I. KOLBANEV, P. UL'YANOVA, YU. FROLOV, P. BUTYAGIN
Semenov Institute of Chemical Physics, Russian Academy of Science, Moscow, Russia
E-mail: alla_pivkina@mail333.com

J. SCHOONMAN
Delft Institute for Sustainable Energy, Delft University of Technology, DELFT, The Netherlands

Nanocrystalline aluminium powder has been prepared by high-energy ball milling of flaked micron-sized aluminium powder in the presence of 10 wt% of graphite under argon atmosphere. The structure and chemical composition of as-prepared nanocomposites and the their thermally induced changes are studied by X-ray diffraction (XRD), transmission electron microscopy (TEM), and simultaneous TG-DTA technique (SDT). TEM studies reveal that the aluminum nanoparticles have a size of 20–50 nm and they are randomly distributed within graphite "threads," which in turn form aggregates of 3–5 μm. The oxidation behaviour of nano-Al in air was studied and compared to a precursor mixture of Al powder with average particle size of 21 μm and 10 wt% of graphite. For both powders, two stages of oxidation were observed in the temperature range 500–660°C and beyond 750°C. The mass gain for the first oxidation stage of the nano-powder is 3.5 times higher than that of the micron-sized one. A decrease of the activation energy of Al oxidation has been found for the nano-Al powder in comparison to the precursor aluminium. The evolution of crystal structure of aluminium oxide during oxidation of the Al/C composite powder has been followed by XRD.

1. Introduction

Nanosized aluminium powder can successfully replace the micron-sized Al powder in propellants [1, 2] to increase the combustion efficiency and to decrease agglomeration of the combustion products. The initial oxidation of Al nanopowder between 400 and 600°C has been observed in [3]. The thermal behaviour of ALEX, a nanosized Al powder produced by the electro-explosion process in nitrogen, helium, and air was evaluated [3].

This paper presents a study of the thermal properties of mechanically activated aluminium nano-powder, including the thermal decomposition parameters, and kinetic parameters of oxidation obtained by TG and DTA techniques.

2. Experimental

Nano-sized aluminium powder was received from the group of Prof. Butyagin (Semenov Institute of Chemical Physics, RAS, Moscow). Micron-sized aluminium powder (PAP-2, GOST 5592-71) blended with 10 wt% of graphite (MGP, specific surface area of 2 m^2/g) was used as a precursor for the mechanical attrition process, which results in nano-sized Al powder. Details of this process have been reported previously [4].

X-ray diffraction patterns were obtained at room temperature using a Rigaku "Geigerflex" X-ray diffractometer, employing Cu K_α radiation. The morphology of the nanocomposites was observed by transmission electron microscope (JEM-2000 EX-II) at 200 kV. Thermogravimetry (TG), derivative thermogravimetry (DTG), and differential thermal analysis (DTA) were carried out using a MOM Q-1500 thermal analyzer.

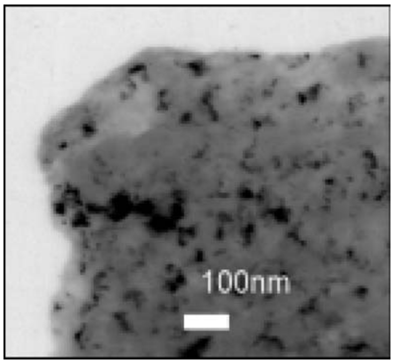

Figure 1 TEM (bright field) image showing Al nanoparticles within the Al/C nanocomposite.

---

*Author to whom all correspondence should be addressed.

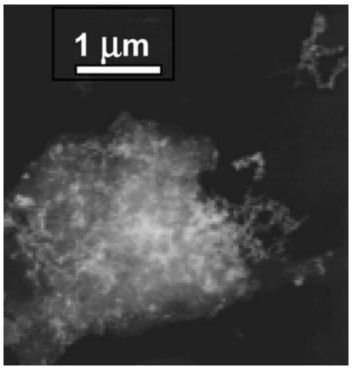

Figure 2 TEM (dark field) image of Al/C nanocomposite showing the aggregation of Al nanoparticles.

3. Results and discussion

TEM studies reveal that the aluminium nanoparticles have a size of 20–50 nm and they are randomly distributed within graphite "threads" (Fig. 1), which in turn form aggregates of 3–5 μm (Fig. 2).

The TG-DTA curves for the two different Al powders taken during the heating in air are shown in Figs 3 and 4, respectively. The thermograms of the powders exhibit several exothermic peaks: one is below the melting point of Al ($\sim$660°C), and second complex exotherm is observed above the melting point. The first mass gain for the micron-sized Al, $\Delta m_1 = 12.5\%$, was observed in the temperature interval 500–660°C. For the nano-sized Al, the mass gain at temperatures below the melting point is much higher, i.e., $\Delta m_1 = 43.5\%$. A second mass gain is observed for metal powders heated in air above 800°C. The second mass gain for micron-sized powder is $\Delta m_2 = 54\%$. For the nano-sized Al powder, the second stage of oxidation shows $\Delta m_2 = 19.8\%$. Table I summarizes the observed experimental data.

A substantial part of nano-sized aluminium is oxidized at temperatures below the Al melting point, whereas for the micron-sized powder this amount is considerably lower. On the contrary, in the temperature range from 800 to 1000°C the amount of oxidised metal is considerably higher for the micron-sized powder.

For the thermal behaviour of aluminium in air, the kinetic parameters determined using different ASTM methods [5, 6] are compared in Table II. The measured values of the activation energy of the initial stage of oxidation of the nano-sized Al powder are smaller than those for the micron-sized powder.

The X-ray diffraction patterns of the Al powders after different stages of oxidation reveal that at temperatures below 740°C, the oxidation process of micron-sized aluminium yields three crystalline phase, i.e., carbon, pure aluminium, and γ-Al_2O_3 (see Table III). After the thermal treatment in the temperature range 20–1000°C, the oxidation products are mostly α-Al_2O_3, metal Al, and γ-Al_2O_3 with a minor amount of θ-Al_2O_3. The thermal treatment of nano-sized activated Al powder at temperatures below 740°C

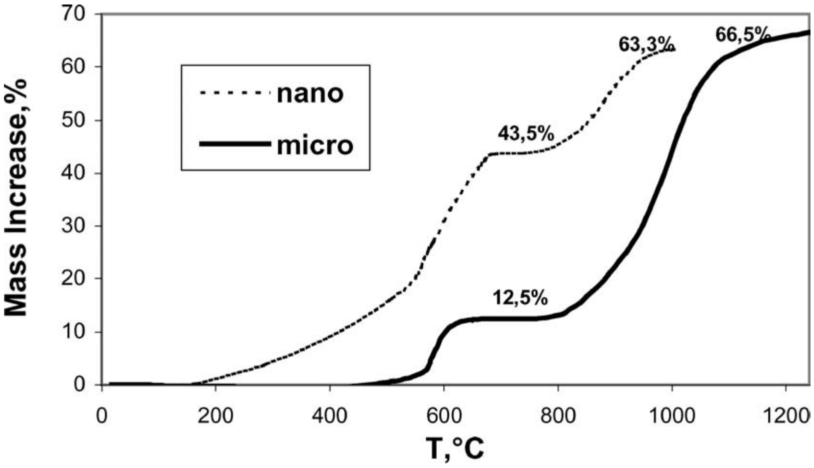

Figure 3 TG curves for micron-sized Al and nano-sized Al powders taken during the heating in air. The heating rate was 10 K/min.

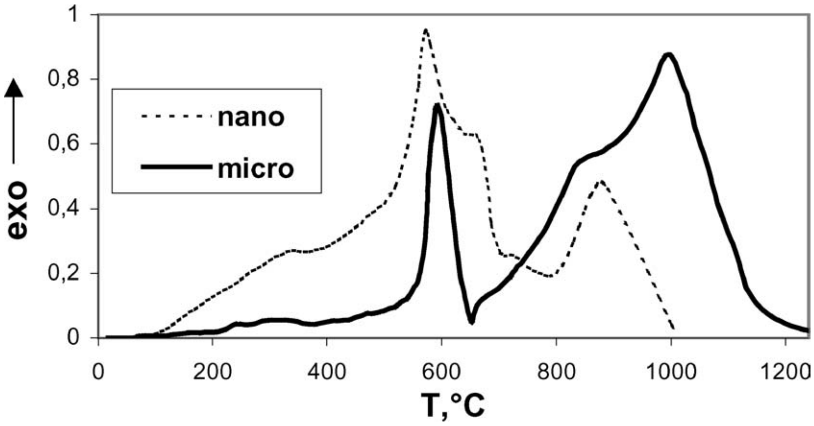

Figure 4 DTA curves for micron-sized Al and nano-sized Al powders taken during the heating in air. The heating rate was 10 K/min.

TABLE I TG results for Al powders of different particle size. The average particle size of the micron-sized powder is 21 μm and of the nano-sized powder 20 nm

Al powder	T_1 (°C)	T_2 (°C)	Δm_1 (%)	Δm_2 (%)	Δm (%)
Micron-sized	500	800	12.5	54.0	66.5
Nano-sized	170	800	43.5	19.8	63.3

Note: T_1 is the temperature of the onset of the first stage of oxidation at which a visible deflection from the established baseline is observed; T_2 is the temperature of the onset of the second stage of oxidation at which a visible deflection from the established baseline is observed; Δm_1 is the mass gain obtained between ~500 and 660°C; Δm_2 is the mass gain obtained above 800°C; the total mass gain $\Delta m = \Delta m_1 + \Delta m_2$.

TABLE II Comparison of the kinetic parameters of the thermal decomposition of Al powder of different particle size

	E (kJ/mol)	
Method	Micron-sized	Nano-sized
TG ASTM E1641	196.8 ± 14.8	127.3 ± 9.5
DTA ASTM E698	165.0 ± 10.7	141.1 ± 9.2

TABLE III The results of the quantitative XRD phase analysis of the powders

		Phase content (wt%)				
Sample	T (°C)	C	Al	γ-Al_2O_3	α-Al_2O_3	θ-Al_2O_3
90%Micron-sized Al/10%C	20	10	90	–	–	–
	740	10	65	20	–	–
	1000	–	9	28	52	11
Nano-sized activated Al	20	10	90	–	–	–
	740	–	24	76	–	–
	1000	–	–	100	–	–

yields predominantly crystalline phases of alumina (γ-Al_2O_3) and pure aluminium. After the oxidation up to 1000°C, no traces of pure aluminium were found, and the presence of γ-Al_2O_3 and θ-Al_2O_3 is observed.

4. Conclusions

Two stages of oxidation were observed at temperatures in the range 500–740°C and below 1000°C for the nano-Al powder and precursor micron-Al powder. The mass gain for the first oxidation stage of the nano-powder is 3.5 times higher than that of the micron-sized powder. A decrease of the activation energy for Al oxidation has been found for the nano-Al powder as compared to that for the precursor aluminium powder. For the activated nano-sized powder, the major part of aluminium was oxidised below 740°C with the formation of γ-Al_2O_3, whereas for the micron-size powder, the major part of aluminium is oxidized in the range of 740–1000°C with predominant formation of α-Al_2O_3.

Acknowledgements

The authors are grateful to the Russian Foundation for Basic Research (RFBR grant #01-03-32530) and to the Netherlands Organization for Scientific Research (NWO grant #047.011) for financial support of the project.

References

1. M. M. MENCH, C. L. YEH and K. K. KUO, in Proceedings of the 29th Int. ICP Conference (Karlsruhe, Germany, June 1998) p. 30/1.
2. V. N. SIMONENKO and V. E. ZARKO, in Proceedings of the 30th Int. ICP Conference (Karlsruhe, Germany, June 1999) p. 21/1.
3. D. E. JONES, P. BROUSSEAU, R. C. FOUCHARD, A. M. TURCOTTE and Q. S. M. KWOK, *J. Therm. Anal. Cal.* **61** (2000) 805.
4. I. V. KOLBANEV, A. N. STRELETSKII and P. YU. BUTYAGIN, *J. Chem. Phys.* **19** (2000) 96 (in Russian).
5. ASTM E1641-94, Standard Test Method for Arrhenius Kinetic Constants for Thermally Unstable Materials, American Society for Testing and Materials, Philadelphia, PA, USA.
6. ASTM E698-79 (Reapproved 1993), Standard Test Method for Arrhenius Kinetic Constants for Thermally Unstable Materials, American Society for Testing and Materials, Philadelphia, PA, USA.

Received 11 September 2003
and accepted 27 February 2004